1990ApJ...363..154B

THE ASTROPHYSICAL JOURNAL, 363:154–158, 1990 November 1
© 1990. The American Astronomical Society. All rights reserved. Printed in U.S.A.

IMAGES IN THE ROCKET ULTRAVIOLET: YOUNG CLUSTERS IN H II REGIONS OF M83

RALPH C. BOHLIN
Space Telescope Science Institute
ROBERT H. CORNETT AND JESSE K. HILL
ST Systems Corporation
AND
THEODORE P. STECHER
Laboratory for Astronomy and Solar Physics, NASA/Goddard Space Flight Center
Received 1990 February 5; accepted 1990 April 26

ABSTRACT

UV images of M83 at 1540 and 2360 Å reveal 18 compact sources that are associated with H II regions. $E(B-V)$ values were estimated individually from the observed UV and optical colors and the Galactic UV extinction curve, using theoretical flux distributions. The dereddened colors are consistent with ages up to 3×10^6 yr. A maximum possible age of 6.5×10^6 yr is obtained assuming foreground reddening only. The distribution of observed colors is consistent with the Galactic reddening curve but not with enhanced far-UV extinction, as in the LMC 30 Dor curve. The Hα fluxes suggest either that dust within the H II regions absorbs up to 70% of the Lyman continuum radiation or that a similar fraction of the Hα flux is below the surface brightness detection limit. Cluster mass estimates depend on the range of stellar masses present but are probably in the range 10^4–10^5 $M_{\odot}$.

Subject headings: clusters: open — galaxies: individual (M83) — galaxies: interstellar matter — nebulae: H II regions — ultraviolet: general

I. INTRODUCTION

Young populous clusters that are apparently similar in mass and structure to the old globular clusters of the Galaxy are well-known constituents of the Magellanic clouds. M31 also contains some young globulars (Bohlin *et al.* 1988). Ages in the range 10^7–10^8 yr have been estimated for these clusters on the basis of observed global cluster colors, and also from observations of individual stars of the LMC clusters (Elson and Fall 1988; Bohlin *et al.* 1988). The identification of populous clusters at an even earlier stage of evolution, where main-sequence O stars are present, would be of great interest. A natural place to look for such clusters is the nearby galaxy M83, which has a nuclear starburst (Bohlin *et al.* 1983*b*) and a high supernova rate (Richter and Rosa 1989).

The SAB(s) I–II galaxy M83 (NGC 5236) was observed 1982 April 17 by our rocket-borne prototype of the Ultraviolet Imaging Telescope, to be flown on the Space Shuttle Spacelab Astro Mission (Stecher *et al.* 1984). Bohlin *et al.* (1983*b*) reported an investigation of the bright nuclear starburst, using UV images obtained in both the CsTe band (effective wavelength 2360 Å) and the CsI band (effective wavelength 1540 Å), as well as *IUE* spectra from the SWP and LWR cameras. In this article, UV image data in the CsTe and CsI bands and the *B* and *V* band optical images of Talbot, Jensen, and Dufour (1979, hereafter TJD) are used to investigate young star clusters associated with H II regions in the spiral arms.

II. OBSERVATIONS AND DATA REDUCTION

Plots of the bandpass response curves and a description of the 38 cm rocket telescope and the UV detectors are given in Table 1 of Bohlin *et al.* (1985). The UV photons were detected on the photocathodes (either CsTe or CsI) of the UV camera microchannel plate image intensifiers, which were fiber-optically coupled to Kodak IIa-O 70 mm film. The film was digitized using a PDS 1010a microdensitometer. The density images were linearized using a characteristic curve derived by requiring that the M83 flight data and the M5 data obtained on the same flight give consistent photometric results for a set of three exposures per field, over a dynamic range of 25 in exposure time. Laboratory exposures provided the flat fields.

The absolute calibrations of both the CsTe and CsI cameras were determined from *IUE* spectra of the M83 nuclear starburst (Bohlin *et al.* 1983*b*) and the M5 UV bright star (Bohlin *et al.* 1983*a*) integrated over the UV bandpasses. The absolute calibration of the optical frames is given by TJD.

III. H II REGIONS

Using the Hα image data of TJD, de Vaucouleurs, Pence, and Davoust (1983) identified 60 H II regions in M83 and tabulated their positions, isophotal areas, and Hα fluxes.

The positions of the H II regions were inspected on each of the continuum images. Many of the H II regions were found to be positionally coincident with unresolved or barely resolved optical and UV sources. After measuring aperture magnitudes for these sources on the near-UV (CsTe photocathode) and far-UV (CsI photocathode) images, and on the *B* and *V* band images of TJD, the 18 brightest sources in *V* were selected for further analysis. Apertures of radius 10″.8 were used on the UV images and 3″.6 on the optical images; the aperture radii differ because of the broader point spread function of the UV images. The selected H II regions are located in spiral arms 1.0–3.5 kpc from the nuclus. The corresponding optical and UV sources are candidates for young populous clusters containing the main-sequence O stars exciting the H II regions.

Figure 1*a* (Plate 4) shows the near-UV (CsTe) 25 s exposure of M83, with the positions of the 18 H II selected regions circled. Figure 1*b* (Plate 5) shows the far-UV (CsI) 25 s exposure. (The *B* and *V* band images are shown in Fig. 1 of TJD.)

© American Astronomical Society • Provided by the NASA Astrophysics Data System

1990ApJ...363..154B

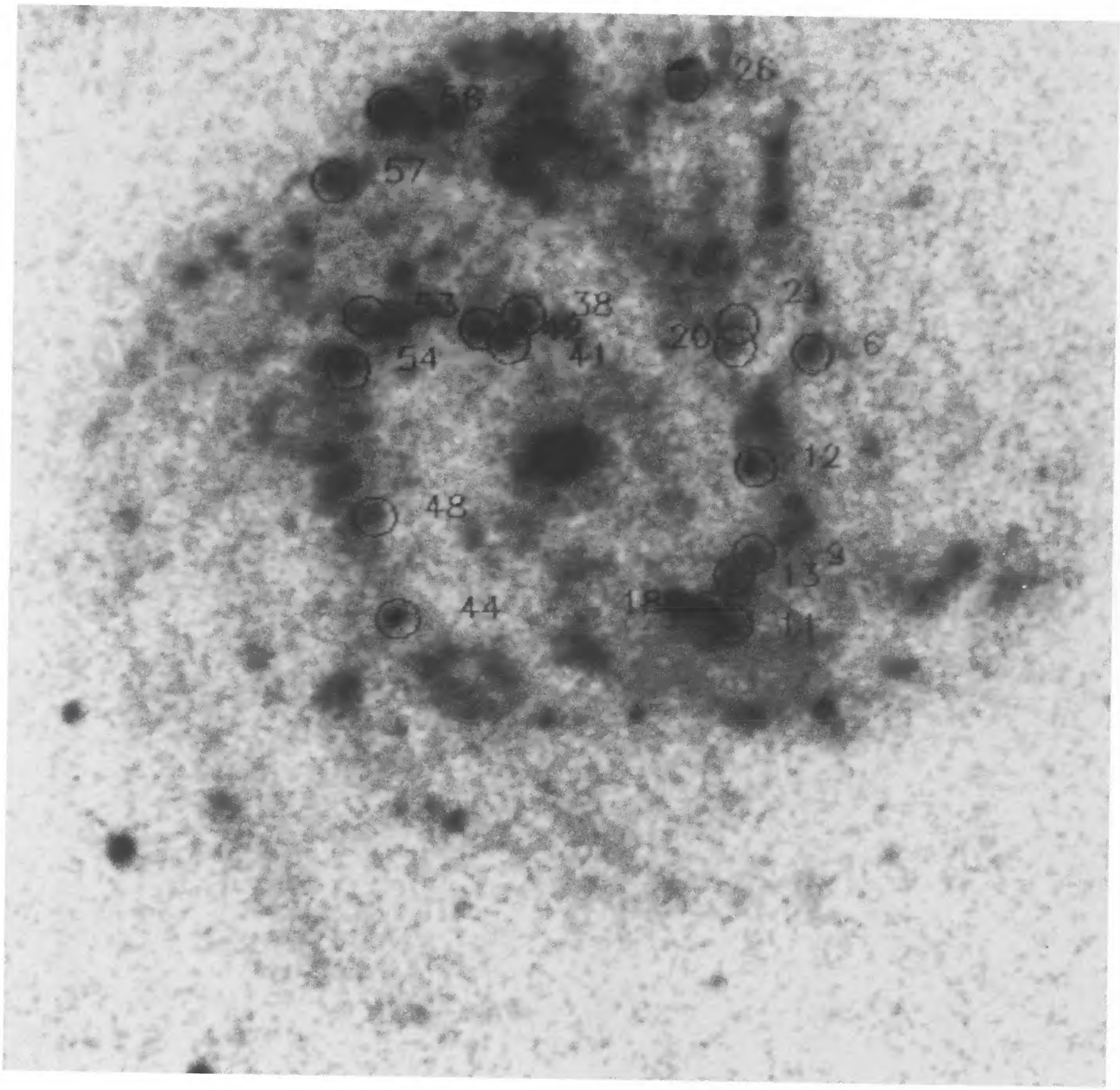

FIG. 1*a*

FIG. 1.—UV sounding rocket images of M83 in 10′ × 10′ fields. North is 10°8 clockwise from the top, and east is a similar angle from the left. The 18 H II regions are circled. Numbers are from de Vaucouleurs, Pence, and Davoust (1983); (*a*) near-UV (2360 Å CsTe band), (*b*) far-UV (1540 Å CsI band).

BOHLIN *et al.* (*see* **363**, 154)

© American Astronomical Society • Provided by the NASA Astrophysics Data System

1990ApJ...363..154B

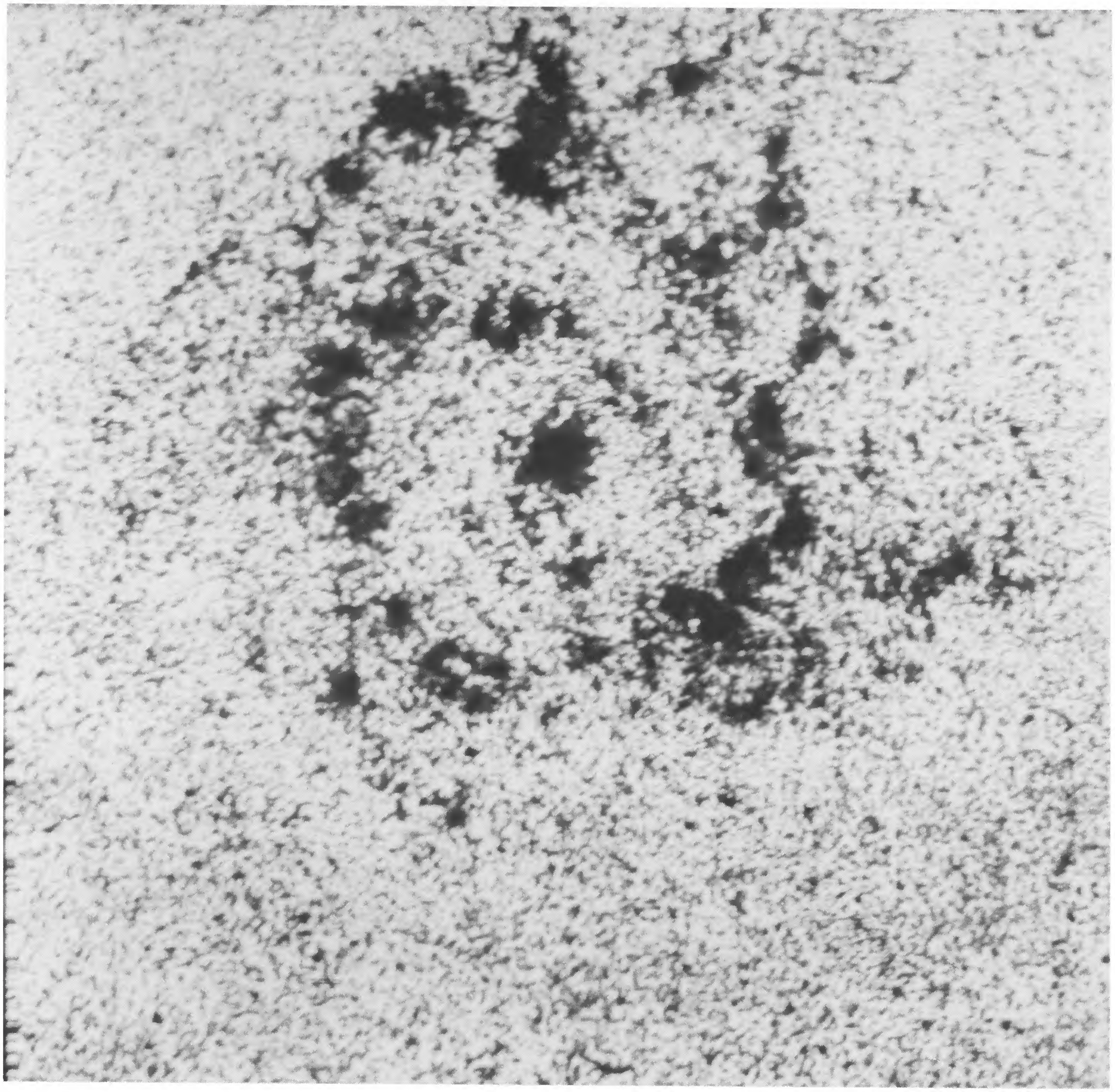

BOHLIN *et al.* (*see* **363**, 154)

© American Astronomical Society • Provided by the NASA Astrophysics Data System

1990ApJ...363..154B

TABLE 1

H II REGION PHOTOMETRY

ID	V	$B-V$	F_{fuv} [ergs (cm^2 Å s)$^{-1}$]	F_{nuv} [ergs (cm^2 Å s)$^{-1}$]	$m_{fuv}-V$	$m_{nuv}-V$
6	16.45	−0.12	1.29×10^{-14}	4.63×10^{-15}	−2.83	−1.72
9	16.20	−0.02	1.37×10^{-14}	4.97×10^{-15}	−2.63	−1.54
11	15.67	0.04	1.68×10^{-14}	6.96×10^{-15}	−2.34	−1.38
12	16.10	0.03	1.29×10^{-14}	4.35×10^{-15}	−2.48	−1.30
13	16.34	−0.02	1.93×10^{-14}	6.01×10^{-15}	−3.16	−1.89
18	16.37	−0.13	1.54×10^{-14}	5.70×10^{-15}	−2.94	−1.86
20	17.18	0.11	4.67×10^{-15}	2.21×10^{-15}	−2.45	−1.64
21	17.30	0.17	7.24×10^{-15}	1.93×10^{-15}	−3.04	−1.61
26	16.62	−0.08	1.45×10^{-14}	4.56×10^{-15}	−3.12	−1.86
38	16.55	−0.07	1.70×10^{-14}	5.46×10^{-15}	−3.22	−1.99
41	16.58	0.06	1.73×10^{-14}	5.00×10^{-15}	−3.27	−1.93
42	15.87	−0.25	1.43×10^{-14}	5.49×10^{-15}	−2.36	−1.32
44	16.36	−0.11	1.68×10^{-14}	3.70×10^{-15}	−3.02	−1.38
48	17.16	−0.09	1.25×10^{-14}	2.71×10^{-15}	−3.50	−1.84
53	17.29	0.02	1.45×10^{-14}	5.87×10^{-15}	−3.79	−2.82
54	15.83	−0.18	1.90×10^{-14}	5.27×10^{-15}	−2.63	−1.24
56	16.95	−0.38	2.87×10^{-14}	7.96×10^{-15}	−4.19	−2.80
57	17.16	−0.27	2.17×10^{-14}	5.06×10^{-15}	−4.09	−2.52

Registered versions of the images were created using the UIT MOUSSE interactive image processing system (Pfarr *et al.* 1988), which was also used to perform the aperture photometry. The identification numbers from de Vaucouleurs, Pence, and Davoust (1983), the V aperture magnitudes, $B-V$ colors, the near-UV and far-UV aperture fluxes, and the $m_{nuv} - V$ and $m_{fuv} - V$ colors of the 18 H II region sources are given in Table 1. Magnitudes m were computed from fluxes f using the relation $m = -2.5 \log f - 21.10$.

IV. REDDENING, AGE, AND MASS OF THE CLUSTERS

Model spectra appropriate for young clusters were constructed by combining the evolutionary stellar models of Maeder and Meynet (1987, 1988) with the model atmospheres of Kurucz (1979), using a procedure similar to that of Lequeux *et al.* (1981), who used a different set of evolutionary models. Colors were computed using the UV filter curves determined in the laboratory (Bohlin *et al.* 1985) and the optical filter curves from Buser and Kurucz (1978). The initial mass function employed was a power law, with the number of stars per logarithmic mass interval varying with the -1.5 power of the mass for masses ranging from 1.8 to 120 solar masses. Models were calculated for ages ranging from 0–9 $\times 10^6$ yr. Table 2 gives the resulting model $B-V$, $m_{fuv} - V$, $m_{nuv} - V$, and $m_{fuv} - m_{nuv}$ colors. The far-UV luminosity per solar mass and the Lyman continuum photon luminosity per solar mass are also given.

The model colors are plotted versus model age in Figure 2. The model results indicate that all colors are nearly constant for ages up to 4×10^6 yr, but that the colors become significantly redder for larger ages. A temporary excursion to the blue, due to the appearance of luminous blue supergiants and Wolf-Rayet stars, occurs at age 6×10^6 yr.

In order to properly deredden the observed fluxes from extended sources such as H II regions and star clusters, it is necessary to take into account the details of the spatial distribution of the dust, as done by, e.g., Mathis (1983) or Caplan and Deharveng (1986). van der Hulst *et al.* (1988) found, from an analysis of Balmer line and radio continuum photometry of H II regions in M51, that a simplified model including only foreground extinction, extinction from a homogeneous screen outside the H II region, and a modest amount of gray extinction by opaque filaments was sufficient to describe their observations. We have effectively adopted an equivalent model for the extinction of the M83 sources, except that since we have not measured the radio continuum fluxes, we have no estimate for the amount of clumped gray extinction. The $E(B-V)$ values we obtain below from our observed colors would thus lead to lower limits for the actual dust column densities.

Figure 3 is a color-color plot illustrating the observed corre-

TABLE 2

YOUNG CLUSTER MODELS

Age (10^6 yr)	$B-V$	$m_{fuv}-V$	$m_{fuv}-m_{nuv}$	$m_{nuv}-V$	N_{lyc} ($10^{45}\ M_\odot^{-1}$)	L_{fuv} [10^{32} ergs (Å s)$^{-1}\ M_\odot^{-1}$]
0	−0.28	−4.40	−1.42	−2.99	70.3	17.1
1	−0.28	−4.41	−1.40	−3.00	74.6	19.3
2	−0.28	−4.39	−1.37	−3.02	74.3	24.8
3	−0.28	−4.29	−1.31	−2.98	73.5	34.9
4	−0.26	−4.11	−1.25	−2.86	49.8	24.4
5	−0.16	−3.33	−1.25	−2.08	26.9	16.7
6	0.01	−3.58	−1.24	−2.34	12.2	16.4
7	0.34	−2.12	−1.16	−0.96	2.3	12.5
8	0.33	−2.03	−1.19	−0.84	1.3	10.0
9	0.50	−2.20	−1.22	−0.98	0.9	7.9

© American Astronomical Society • Provided by the NASA Astrophysics Data System

1990ApJ...363..154B

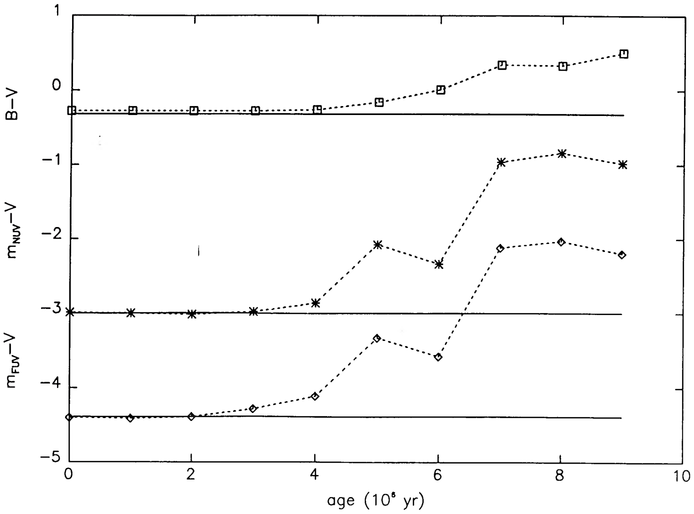

FIG. 2.—$(B-V)$ (*boxes*), $m_{\rm nuv} - V$ (*asterisks*), and $m_{\rm fuv} - V$ (*diamonds*), for the cluster models vs. age. The horizontal solid lines plotted with each model curve are the mean observed colors after dereddening.

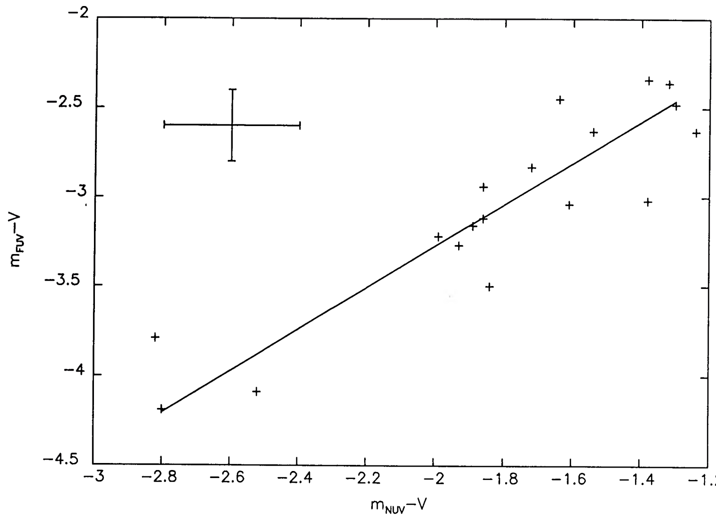

FIG. 3.—$m_{\rm nuv} - V$ vs. $m_{\rm fuv} - V$ for the 18 H II region sources, with a least-squares linear fit. The error bar shows the typical rms photometric error in both colors (0.2 mag).

lation between $m_{\rm nuv} - V$ and $m_{\rm fuv} - V$. The observed variation of both colors is probably due primarily to variations in $E(B-V)$. The observed rms scatter of both colors (about 0.5 mag) is much larger than expected from observational errors (about 0.1 mag in V and 0.2 mag for $m_{\rm fuv}$ and $m_{\rm nuv}$). The observed correlation between the observed $m_{\rm nuv} - V$ and $m_{\rm fuv} - V$ cannot be explained by large errors in V dominating errors in both $m_{\rm fuv}$ and $m_{\rm nuv}$, since the V band magnitudes are expected to be the most precise of the three.

The least-squares linear fit to the observed points in the $m_{\rm nuv} - V$ versus $m_{\rm fuv} - V$ diagram is also shown in Figure 3. The slope of the line is 1.18 ± 0.13, consistent with the value 1.12 predicted by the Galactic reddening curve (Savage and Mathis 1979). According to the models, $m_{\rm nuv} - V$ colors for clusters with ages up to 3×10^6 yr equal -2.99 ± 0.02, while $m_{\rm fuv} - V$ colors redden by 0.12 over the first 3×10^6 yr. Clusters with larger ages are unlikely to be associated with prominent H II regions, since the Lyman continuum luminosity will have declined significantly for ages greater than about 5×10^6 yr, according to Table 2. We estimated $E(B-V)$ for the clusters individually by comparing the observed $m_{\rm nuv} - V$ colors with the model colors for clusters of age 3×10^6 yr or less. The constancy of this color for young clusters, together with the Galactic reddening curve, gives the relation $E(B-V) = [2.99 + (m_{\rm nuv} - V)]/4.67$. The resulting $E(B-V)$ values were used to compute dereddened $B-V$, $m_{\rm fuv} - V$, and $m_{\rm fuv} - m_{\rm nuv}$ colors for the 18 observed clusters. (The dereddened $m_{\rm nuv} - V$ colors are all equal to -2.99.) The dereddened colors and the $E(B-V)$ values are given in Table 3.

A linear fit to the theoretical $m_{\rm nuv} - V$ versus $m_{\rm fuv} - V$ relation implied by the entries for ages up to 9×10^6 yr in Table 2 gives a slope of 1.08, also consistent with the observed slope before dereddening. Thus, part of the observed color variation in $m_{\rm nuv} - V$ could be caused by a larger range in ages past 3×10^6 yr. As mentioned earlier, however, the fact that the Lyman continuum luminosity decreases strongly with age (see Table 2) argues that most of the observed color variation is attributable to variations in the extinction. An upper limit to

TABLE 3

DERIVED CLUSTER PROPERTIES

ID	$E(B-V)$	$(B-V)_0$	$(m_{\rm fuv} - V)_0$	$(m_{\rm fuv} - m_{\rm nuv})_0$	Mass ($M_\odot$)	$Ly_{\rm pred}$ (10^{50} s^{-1})	$Ly_{\rm ob}/Ly_{\rm pred}$
6	0.27	−0.40	−4.26	−1.26	8.2×10^4	26.8	0.40
9	0.31	−0.30	−4.27	−1.27	8.2×10^4	26.7	0.04
11	0.35	−0.30	−4.15	−1.15	1.2×10^5	37.5	0.20
12	0.36	−0.34	−4.38	−1.38	6.1×10^4	19.8	1.39
13	0.24	−0.26	−4.40	−1.40	8.4×10^4	27.5	0.38
18	0.24	−0.38	−4.21	−1.21	8.8×10^4	28.9	0.22
20	0.29	−0.18	−3.97	−0.97	2.0×10^4	6.7	1.25
21	0.30	−0.13	−4.60	−1.60	3.7×10^4	12.2	0.20
26	0.24	−0.32	−4.39	−1.39	7.8×10^4	25.4	0.04
38	0.22	−0.29	−4.35	−1.35	1.1×10^5	34.4	0.07
41	0.23	−0.17	−4.47	−1.47	1.1×10^5	35.7	0.17
42	0.36	−0.61	−4.24	−1.24	8.9×10^4	29.0	0.67
44	0.35	−0.46	−4.83	−1.83	9.2×10^4	30.2	0.04
48	0.25	−0.34	−4.79	−1.79	6.6×10^4	21.5	0.16
53	0.04	−0.02	−4.00	−1.00	7.0×10^4	22.8	0.09
54	0.38	−0.56	−4.60	−1.60	1.1×10^5	35.3	0.08
56	0.04	−0.42	−4.41	−1.42	1.5×10^5	48.4	0.05
57	0.10	−0.37	−4.63	−1.64	1.1×10^5	34.5	0.06

© American Astronomical Society • Provided by the NASA Astrophysics Data System

1990ApJ...363..154B

the cluster ages can be estimated from the maximum value of $m_{\mathrm{nuv}} - V$, dereddened using the foreground extinction $E(B-V) = 0.08$ from de Vaucouleurs, de Vaucouleurs, and Corwin (1976) only, and compared with the intrinsic colors as a function of age in Table 2. The limiting dereddened value of $m_{\mathrm{nuv}} - V$ so obtained is -1.61, implying, from the entries in Table 2, a maximum age of about 6.5×10^6 yr.

Since the standard deviation of the dereddened $m_{\mathrm{fuv}} - V$ colors is 0.23 mag, the individual $E(B-V)$ values should be accurate to about ± 0.05. Since the mean $E(B-V)$ we obtain is 0.25, while the foreground Galactic value has been estimated at about 0.08, we conclude that at least about 70% of the extinction takes place within M83. The agreement of the slope of the fitted line in Figure 3 with that predicted by the Galactic reddening curve implies that the reddening curve within M83 is like that in the Galaxy, rather than a curve with enhanced far-UV extinction like that in the 30 Dor region of the LMC, which would lead to a predicted slope about 1.6 for the fitted line (Fitzpatrick 1985).

The model colors were compared with the mean colors of the 18 M83 H II region sources after dereddening appropriately. The mean dereddened colors are $\langle B-V \rangle = -0.32 \pm 0.03$, $\langle m_{\mathrm{fuv}} - m_{\mathrm{nuv}} \rangle = -1.39 \pm 0.06$, and $\langle m_{\mathrm{fuv}} - V \rangle = -4.39 \pm 0.06$, where the quoted errors are the expected error in the mean for the 18 clusters. Since the observed scatter in the dereddened $B-V$, $m_{\mathrm{fuv}} - V$, and $m_{\mathrm{fuv}} - m_{\mathrm{nuv}}$ colors is consistent with expected observational scatter, only the mean colors are used in the comparison with the models.

Acording to Table 2, the mean dereddened colors fit best the 2×10^6 yr old cluster model, although all ages from 0–3×10^6 give model colors consistent with the observations within $\pm 2\ \sigma$. We have calculated masses for the clusters from the dereddened far-UV fluxes and the model far-UV luminosity per solar mass for a two million year old cluster. The masses obtained are in the range 10^4–$10^5\ M_{\odot}$, similar to masses estimated for the young globular clusters of the LMC by Freeman (1980). The computed masses are given in Table 3. Actual masses could be higher if extinction by totally opaque filaments is significant. The 0–3×10^6 yr range of allowable ages alone leads to a $\pm 50\%$ range in allowable cluster mass.

Masses were computed assuming the model clusters to have mass functions extending to masses only as low as 1.8 $M_{\odot}$, where the IMF used by Lequeux *et al.* (1981) has a break in slope. The measured optical and UV fluxes are not directly sensitive to the presence of lower mass stars. Lequeux *et al.* (1981) use a power-law IMF for masses above 1.8 $M_{\odot}$, with a break in slope to -0.6 for lower masses down to 0.007 $M_{\odot}$. The addition of lower mass stars to our IMF would lead to larger cluster mass estimates by a factor of ~ 3.

If stars of all masses are present, the observed sources may well be the evolutionary forebears of clusters comparable to the young LMC populous clusters or the apparently young globulars in M31 (Bohlin *et al.* 1988). Although very young populations formed in Galactic spiral arm giant molecular cloud complexes are dominated by massive stars, considerable low-mass star formation occurs also (Boss 1989). The cluster models could be constrained more narrowly when more precise visual and UV photometry become available. The mass function and range question could also be further investigated using high-resolution imagery in the optical and UV bands to probe the structure of the clusters, which are undoubtedly not yet relaxed. High-resolution optical or UV spectroscopy could lead to mass estimates from the velocity dispersions. Infrared photometry and spectroscopy could also be used to search for evidence for the presence of low-mass stars.

Lyman continuum photon luminosities per solar mass are also predicted by the cluster models. The Hα fluxes measured by de Vaucouleurs, Pence, and Davoust (1983) were used to estimate Lyman continuum luminosities for the clusters after dereddening using the extinctions determined from the $m_{\mathrm{nuv}} - V$ colors and assuming that 0.5 of all Lyman continuum photons lead to an Hα recombination photon (Spitzer 1978). The extinction is assumed to take place outside the H II region, so the extent of the Strömgren sphere is not affected. If $\mathrm{Ly_{ob}}$ is the Lyman continuum luminosity inferred from the observed Hα flux and $\mathrm{Ly_{pred}}$ is the Lyman continuum luminosity predicted for a cluster of age 2×10^6 yr with the mass inferred from the far-UV flux, the average value of $\mathrm{Ly_{ob}}/\mathrm{Ly_{pred}}$ is 0.31.

Since the Hα fluxes reported by de Vaucouleurs, Pence, and Davoust (1983) are surface brightness limited, the discrepancy between the observed and predicted Hα fluxes could be explained if most of the Hα emission is actually from low surface brightness regions below their threshold. Also, much of the extinction inferred from the observed $m_{\mathrm{nuv}} - V$ colors may take place within the H II regions, thereby decreasing the Lyman continuum flux available for ionizing hydrogen. An independent estimate of the Lyman continuum flux could be made using thermal radio fluxes determined for the same H II regions for which Hα fluxes have been measured. A comparison with Hα fluxes would also allow independent estimates of $E(B-V)$. The Lyman continuum luminosities determined from the best-fit age of 2×10^6 yr and the mass determined from the far-UV flux are given in Table 3, with the ratio of the observed Hα flux to that expected for a cluster of age 2×10^6 yr with the inferred mass.

More sophisticated models for the dust distribution and extinction correction could be considered, if radio continuum fluxes, Hα and Hβ fluxes were measured for equivalent spatial areas, as done by van der Hulst *et al.* (1988) in the case of M51, and Caplan and Deharveng (1986), in the case of the LMC.

We are grateful to the Sounding Rocket staff at Goddard Space Flight Center for their essential assistance in obtaining the data for this article and to Reginald Dufour for providing copies of the optical images of M83. This research was supported under NASA RTOP 680-879-11-41 and NASA Spacelab Project 680-440-51-02.

REFERENCES

Bohlin, R. C., Cornett, R. H., Hill, J. K., Hill, R. S., O'Connell, R. W., and Stecher, T. P. 1985, *Ap. J.* (*Letters*), **298**, L37.
Bohlin, R. C., Cornett, R. H., Hill, J. K., Hill, R. S., and Stecher, T. P. 1988, *Ap. J.*, **334**, 657.
Bohlin, R. C., Cornett, R. H., Hill, J. K., Smith, A. M., and Stecher, T. P. 1985, *Ap. J.*, **292**, 687.
———. 1983*b*, *Ap. J.* (*Letters*), **274**, L53.
Bohlin, R. C., Cornett, R. H., Hill, J. K., Smith, A. M., Stecher, T. P., and Sweigart, A. V. 1983*a*, *Ap. J.* (*Letters*), **267**, L89.
Boss, A. P. 1989, *Pub. A.S.P.*, **101**, 767.
Buser, R., and Kurucz, R. L. 1978, *Astr. Ap.*, **70**, 555.
Caplan, J., and Deharveng, L. 1986, *Astr. Ap.*, **155**, 297.
de Vaucouleurs, G., de Vaucouleurs, A., and Corwin, H. G. 1976, *Second Reference Catalogue of Bright Galaxies* (Austin: University of Texas Press).

© American Astronomical Society • Provided by the NASA Astrophysics Data System

1990ApJ...363..154B

de Vaucouluers, G., Pence, W. D., and Davoust, E. 1983, *Ap. J. Suppl.*, **53**, 17.
Elson, R. A. W., and Fall, S. M. 1988, *A.J.*, **96**, 1383.
Fitzpatrick, E. L. 1985, *Ap. J.*, **299**, 219.
Freeman, K. 1980, in *IAU Symposium 85, Star Clusters*, ed. J. E. Hesser (Dordrecht: Reidel), p. 317.
Kurucz, R. L. 1979, *Ap. J. Suppl.*, **40**, 1.
Lequeux, J., Maucherat-Joubert, M., Deharveng, J. M., and Kunth, D. 1981, *Astr. Ap.*, **103**, 305.
Maeder, A., and Meynet, G. 1987, *Astr. Ap.*, **182**, 243.
———. 1988, *Astr. Ap. Suppl.*, **76**, 411.
Mathis, J. S. 1983, *Ap. J.*, **267**, 119.
Pfarr, B. B., Hill, J. K., Hill, R. S., and Landsman, W. B. 1988, *Bull. AAS*, **20**, 709.
Richter, O-G., and Rosa, M. 1989, *Astr. Ap.*, **206**, 219.
Savage, B. D., and Mathis, J. S. 1979, *Ann. Rev. Astr. Ap.*, **17**, 73.
Spitzer, L. 1978, *Physical Processes in the Interstellar Medium* (New York: Wiley).
Stecher, T. P., Bohlin, R. C., O'Connell, R. W., Roberts, M. S., Smith, A. M., and Parise, R. A. 1984, *Bull. AAS*, **16**, 905.
Talbot, R. J., Jensen, E. B., and Dufour, R. J. 1979, *Ap. J.*, **229**, 91 (TJD).
van der Hulst, J. M., Kennicutt, R. C., Crane, P. C., and Rots, A. H. 1988, *Astr. Ap.*, **195**, 38.

RALPH C. BOHLIN: Space Telescope Science Institute, Homewood Campus, Baltimore, MD 21218

ROBERT H. CORNETT and JESSE K. HILL: ST Systems Corporation, 4400 Forbes Boulevard, Lanham, MD 20706

THEODORE P. STECHER: Laboratory for Astronomy and Solar Physics, NASA/Goddard Space Flight Center, Code 680, Greenbelt, MD 20771

© American Astronomical Society • Provided by the NASA Astrophysics Data System